NONLINEAR DIGITAL AND PULSE-WIDTH ATTITUDE CONTROL OF INFORMATION MINI-SATELLITES

Yevgeny Somov
Research Institute for Problems
of Mechanical Systems Reliability
Samara State Technical University
Russia
e_somov@mail.ru

Sergey Butyrin
Research Institute for Problems
of Mechanical Systems Reliability
Samara State Technical University
Russia
butyrinsa@mail.ru

Sergey Somov
Research Institute for Problems
of Mechanical Systems Reliability
Samara State Technical University
Russia
s_somov@mail.ru

Abstract
The information mini-satellites (for communication, geodesy, radio- and opto-electronic observation of the Earth et al.) have some principle problems with respect to their spatial attitude guidance and control. In the paper these problems are considered and obtained results are presented.

Key words
Spacecraft dynamics, nonlinear attitude control

1 Introduction

Contemporary small information spacecraft today are applied for communication (Fig. 1), geodesy, radio- and opto-electronic (Fig. 2) observation of the Earth et al. (Kramer, 2002; Helvajian and Jonson, 2009). The information mini-satellites are applied at the orbit altitudes from 550 up to 1500 km, they have mass up to 500 kg and their structure consist the large-scale solar array panels (SAPs), Figs. 1 & 2, for an energy supplying of the electro-reaction engines (Somov, 2007, 2010, 2012*a*,*b*). The programmed guidance of the land-survey spacecraft (SC) is presented by a consequence of the observation intervals for a target application – the courses and the intervals of spatial rotational maneuvers. In the paper we consider the optimization problem on spatial attitude guidance of such SC and in answer to new challenges on stability and control in aerospace (Somov, Ye. *et al.*, 2012) we present elaborated methods and some results on dynamic synthesis of the SC attitude robust digital control by the gyro moment cluster (GMC) with three gyrodines (GDs) and the pulse-width control by the combine electro-reaction unit (CEU) with 8 electro-reaction engines (EREs).

2 Mathematical Models

We use the inertial reference frame (IRF) $\mathbf{I}$, the orbit reference frame (ORF) $\mathbf{O}$ ($\mathrm{O}x^{\mathrm{o}}y^{\mathrm{o}}z^{\mathrm{o}}$) and standard defined the SC body reference frame (BRF) $\mathbf{B}$ ($\mathrm{O}xyz$). The BRF attitude with respect to the IRF $\mathbf{I}$ is defined by quaternion $\mathbf{\Lambda} = (\lambda_0, \boldsymbol{\lambda}), \boldsymbol{\lambda} = (\lambda_1, \lambda_2, \lambda_3)$, and with respect to the ORF – by column $\boldsymbol{\phi} = \{\phi_i\}$ ($i = 1, 2, 3 \equiv 1 \div 3$) of angles $\phi_1 = \psi$ (yaw), $\phi_2 = \varphi$ (roll) and $\phi_3 = \theta$ (pith) in the sequence $13'2''$.

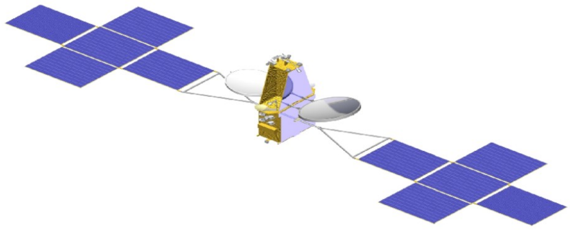

Figure 1. The communication mini-satellite

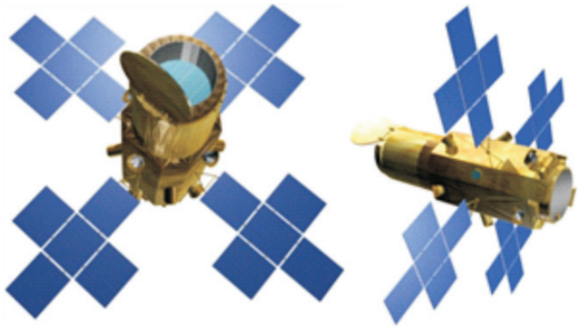

Figure 2. The land-survey mini-satellite, two views

Let us $\mathbf{\Lambda}^p(t)$ is a quaternion and $\boldsymbol{\omega}^p(t) = \{\omega_i^p(t)\}$ is an angular rate vector of the programmed SC body's motion in the IRF. The error quaternion is $\mathbf{E} = (e_0, \mathbf{e}) = \tilde{\mathbf{\Lambda}}^p(t) \circ \mathbf{\Lambda}$, the *Euler* parameters' vector is $\boldsymbol{\mathcal{E}} = \{e_0, \mathbf{e}\}$ and the attitude error's matrix is $\mathbf{C}_e \equiv \mathbf{C}(\boldsymbol{\mathcal{E}}) = \mathbf{I}_3 - 2[\mathbf{e}\times]\mathbf{Q}_e$, where $\mathbf{Q}_e \equiv \mathbf{Q}(\boldsymbol{\mathcal{E}}) = \mathbf{I}_3 e_0 + [\mathbf{e}\times]$ with $\det(\mathbf{Q}_e) = e_0$. Moreover the angular rate error vector is $\delta\boldsymbol{\omega} = \boldsymbol{\omega} - \mathbf{C}_e\boldsymbol{\omega}^p(t)$. Here and further the symbols $\circ$, $\tilde{\cdot}$ for quaternions, $\langle\cdot,\cdot\rangle, \times, \{\cdot\} \equiv \mathrm{col}(\cdot)$, $[\cdot] \equiv \mathrm{line}(\cdot)$ for vectors and $[\cdot\times]$, $(\cdot)^{\mathrm{t}}$, $\lceil\cdot\rfloor \equiv \mathrm{diag}(\cdot)$ for matrix are conventional denotations.

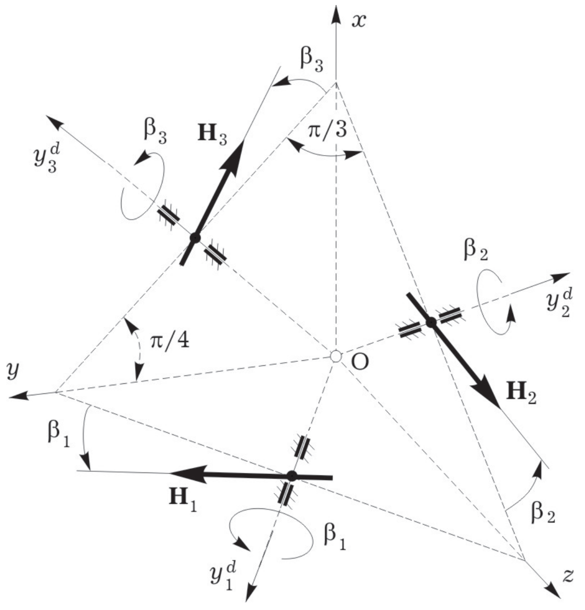

Figure 3. The GMC scheme *Star* by 3 gyrodines

At applied the GMC scheme *Star* (Fig. 3) for a fixed position of *flexible* structures on the SC body with some simplifying assumptions the SC angular motion model is as follows (Somov, Ye., 1992)

$$\dot{\mathbf{\Lambda}} = \mathbf{\Lambda}\circ\boldsymbol{\omega}/2;\quad \mathbf{A}^o\{\dot{\boldsymbol{\omega}},\ddot{\mathbf{q}},\ddot{\boldsymbol{\beta}}\} = \{\mathbf{F}^\omega,\mathbf{F}^q,\mathbf{F}^\beta\}, \qquad (1)$$

$$\mathbf{F}^\omega = \mathbf{M}^{\mathrm{g}} - \boldsymbol{\omega}\times\mathbf{G} + \mathbf{M}^{\mathrm{e}} + \mathbf{M}^d;$$

$$\mathbf{F}^q = \{-a_j^q(\tfrac{\delta^q}{\pi}\Omega_j^q\dot{q}_j + (\Omega_j^q)^2 q_j)\};$$

$$\mathbf{F}^\beta = \mathbf{A}_{\mathrm{H}}^{\mathrm{t}}\boldsymbol{\omega} + \mathbf{M}_b^g + \mathbf{M}_f^g + \mathbf{M}^g;$$

$$\mathbf{A}^o = \begin{bmatrix} \mathbf{J} & \mathbf{D}_q & \mathbf{D}_g \\ \mathbf{D}_q^{\mathrm{t}} & \mathbf{A}^q & \mathbf{0} \\ \mathbf{D}_g^{\mathrm{t}} & \mathbf{0} & \mathbf{A}^g \end{bmatrix};\quad \begin{array}{l} \mathbf{G} = \mathbf{G}^o + \mathbf{D}_q\dot{\mathbf{q}} + \mathbf{D}_g\dot{\boldsymbol{\beta}}; \\ \mathbf{G}^o = \mathbf{J}\,\boldsymbol{\omega} + \boldsymbol{\mathcal{H}}(\boldsymbol{\beta}); \\ \mathbf{A}_{\mathrm{H}}(\boldsymbol{\beta}) = \partial\boldsymbol{\mathcal{H}}(\boldsymbol{\beta})/\partial\boldsymbol{\beta}; \end{array}$$

$$\boldsymbol{\omega} = \{\omega_i\};\ \mathbf{q} = \{q_j\};\ \boldsymbol{\beta} = \{\beta_i\};\ \boldsymbol{\mathcal{H}}(\boldsymbol{\beta}) = \sum \mathbf{H}_i(\beta_i);$$

$$\boldsymbol{\mathcal{H}} = H\begin{bmatrix} -S_1 - aC_2 + aC_3 \\ aC_1 - S_2 - aC_3 \\ -aC_1 + aC_2 - S_3 \end{bmatrix};\ \mathbf{D}_g = J_g a \begin{bmatrix} 0\,1\,1 \\ 1\,0\,1 \\ 1\,1\,0 \end{bmatrix};$$

$$\mathbf{A}_{\mathrm{H}}(\boldsymbol{\beta}) = H\begin{bmatrix} -C_1 & aS_2 & -aS_3 \\ -aS_1 & -C_2 & aS_3 \\ aS_1 & -aS_2 & -C_3 \end{bmatrix};\quad \begin{array}{r} S_i = \sin\beta_i; \\ C_i = \cos\beta_i; \\ a = 1/\sqrt{2}; \end{array}$$

$$\mathbf{A}^q = \lceil a_j^q \rfloor;\ \mathbf{A}^g = J_g\mathbf{I}_3;\ \mathbf{M}_b^g = \{m_{bi}^g\};\ \mathbf{M}_f^g = \{m_{fi}^g\};$$

$$m_{bi}^g = \begin{cases} 0 & |\dot{\beta}_i| \le \dot{\beta}_g^{\mathrm{o}}, \\ b_i^g(\dot{\beta}_i - \dot{\beta}_g^{\mathrm{o}}\,\mathrm{Sign}\dot{\beta}_i) & |\dot{\beta}_i| > \dot{\beta}_g^{\mathrm{o}}; \end{cases}$$

$$m_{fi}^g = \mathrm{Sat}(m_g^{\mathrm{f}}, (\dot{\beta}_i/\dot{\beta}_g^{\mathrm{o}}));\quad \mathbf{M}^g = \{m_i^g(t)\};$$

$$m_i^g(t) = \mathrm{Zh}[\mathrm{Sat}(\mathrm{Qntr}(m_{ik}^g, m_g^{\mathrm{o}}), m_g^{\mathrm{m}}), T_u],$$

where functions $\mathrm{Sat}(x,a)$ and $\mathrm{Qntr}(x,a)$ are general-usage ones, while the holder with the period T_u is of the type: $y(t) = \mathrm{Zh}[x_k, T_u] = x_k\ \forall t \in [t_k, t_{k+1})$, $t_{k+1} = t_k + T_u$, $k \in \mathbb{N}_0 \equiv [0,1,2,\dots)$, vector $\mathbf{M}^{\mathrm{g}} \equiv -\mathbf{A}_{\mathrm{H}}(\boldsymbol{\beta})\dot{\boldsymbol{\beta}}$ is the GMC torque for the SC body attitude control, vector $\mathbf{M}^{\mathrm{e}}$ is torque of the Combine Engine Unit (CEU), see Fig. 4, and vector $\mathbf{M}^d$ presents the external disturbance torques – gravitational, magnetic, by forces of solar pressure et al.

In Fig. 4 the units $\mathbf{e}_p, p = 1 \div 8$ are directed on axes of the electro-reaction engine (ERE) nozzles. Into the BRF these units are presented by columns

$$\mathbf{e}_1 = \{C_\alpha C_\beta, C_\alpha S_\beta, S_\alpha\};\ \mathbf{e}_2 = \{C_\alpha C_\beta, C_\alpha S_\beta, -S_\alpha\};$$

$$\mathbf{e}_3 = \{C_\alpha C_\beta, -C_\alpha S_\beta, S_\alpha\};\quad \mathbf{e}_7 = -\mathbf{e}_2;\quad \mathbf{e}_8 = -\mathbf{e}_1;$$

$$\mathbf{e}_4 = \{C_\alpha C_\beta, -C_\alpha S_\beta, -S_\alpha\};\ \mathbf{e}_5 = -\mathbf{e}_4;\quad \mathbf{e}_6 = -\mathbf{e}_3,$$

where $C_x = \cos x, S_x = \sin x$ with $x = \alpha^{\mathrm{e}}, \beta^{\mathrm{e}}$, Fig. 4. The ERE arrangement points O_p are defined by the radius-vectors $\boldsymbol{\rho}_p$ and are presented into the BRF by columns

$$\boldsymbol{\rho}_1 = \begin{bmatrix} b_x \\ b_y \\ b_z \end{bmatrix};\ \boldsymbol{\rho}_2 = \begin{bmatrix} b_x \\ b_y \\ -b_z \end{bmatrix};\ \boldsymbol{\rho}_3 = \begin{bmatrix} b_x \\ -b_y \\ b_z \end{bmatrix};\ \boldsymbol{\rho}_4 = \begin{bmatrix} b_x \\ -b_y \\ -b_z \end{bmatrix};$$

$$\boldsymbol{\rho}_5 = \begin{bmatrix} -b_x \\ b_y \\ b_z \end{bmatrix};\boldsymbol{\rho}_6 = \begin{bmatrix} -b_x \\ b_y \\ -b_z \end{bmatrix};\boldsymbol{\rho}_7 = \begin{bmatrix} -b_x \\ -b_y \\ b_z \end{bmatrix};\boldsymbol{\rho}_8 = \begin{bmatrix} -b_x \\ -b_y \\ -b_z \end{bmatrix}.$$

Everyone electro-reaction engine have a pulse-width modulation (PWM) of its thrust, moreover command $P^n(t,\tau_r)$ by the thrust inclusion on time τ_r is presented as $P^n(t,\tau_r) \in (0,1)$, namely

$P^n = 1\,\forall t \in [t_r, t_r + \tau_r)\&P^n = 0\,\forall t \in [t_r + \tau_r, t_{r+1})$,

where $r \in \mathbb{N}_0$, $t_{r+1} = t_r + T_u^{\mathrm{e}}$, and the modulation characteristics is described by the ratio

$$\tau_r^{\mathrm{e}} = \begin{cases} 0 & \tau_r < \tau_{\mathrm{m}}; \\ \tau_r & \tau_{\mathrm{m}} \le \tau_r \le T_u^{\mathrm{e}}; \\ T_u^{\mathrm{e}} & \tau_r > T_u^{\mathrm{e}}. \end{cases}$$

Taking into account a transport delay T_{zu}^{e} a dynamic process on the normalized thrust $P_{\mathrm{e}}^n(t)$ is presented by the differential equation $T^{\mathrm{e}}\,\dot{P}_{\mathrm{e}}^n + P_{\mathrm{e}}^n = P^n(t - T_{zu}^{\mathrm{e}}, \tau_r)$ with the initial condition $P_{\mathrm{e}}^n(t_0) = 0$, where a time constant T^{e} accepts two values T_+^{e} or T_-^{e} according to the ratio: $if\ \ P^n = 1\ \ then\ \ T^{\mathrm{e}} = T_+^{\mathrm{e}}\ \ else\ \ T^{\mathrm{e}} = T_-^{\mathrm{e}}$.

Current the ERE thrusts $\mathbf{P}_p(t)$ with fixed units $\mathbf{e}_p$ beginning in the points O_p (see Fig. 4) are presented by the vectors $\mathbf{P}_p(t) = -p_p(t)\mathbf{e}_p$, where $p_p(t) = \mathrm{P}^{\mathrm{m}} P_{\mathrm{e}p}^n(t)$ and P^{m} is a maximal thrust value, identical

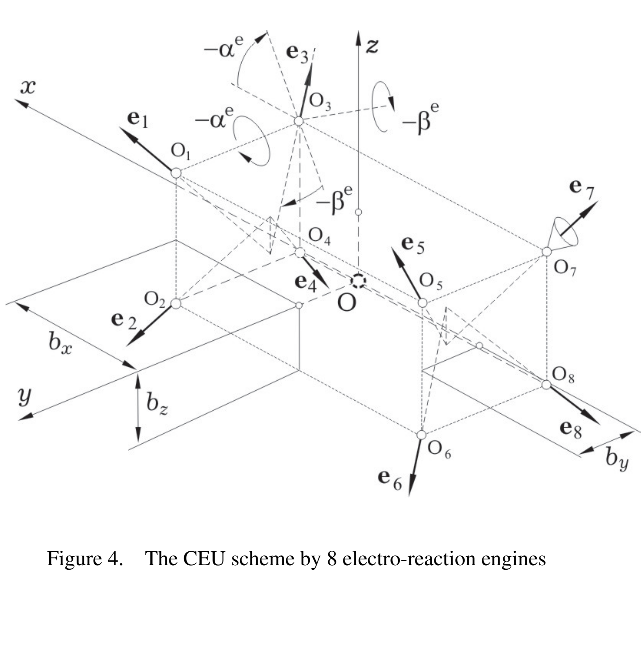

Figure 4. The CEU scheme by 8 electro-reaction engines

for all EREs. The ERE torque vectors $\mathbf{M}_p(t)$ with respect to the point O are calculated by relation $\mathbf{M}_p(t) = [\boldsymbol{\rho}_p\times]\mathbf{P}_p(t)$. In result into the BRF we have the presentations of the CEU force vector $\mathbf{R}^{\rm e}(t) = \Sigma\mathbf{P}_p(t)$ and the CEU torque vector $\mathbf{M}^{\rm e}(t) = \Sigma\mathbf{M}_p(t), p = 1 \div 8$.

Standard denotations are further applied for values of the discrete signals $y(t_k) = y_k$ and $y(t_r) = y_r$ at the time moments $t_k = k\,T_u$ and $t_r = r\,T_u^{\rm e}$. We are assuming that a strap-down inertial navigation system (SINS) is applied for the SC attitude determination into the IRF. The system contains an inertial measuring unit based on the low cost gyro sensors and an astronomical subsystem based on the low cost wide-field-of-view star trackers which are rigidly fixed to the SC body. The SC discrete measured quaternion have the form $\boldsymbol{\Lambda}_k^{\rm m} = \boldsymbol{\Lambda}_k \circ \boldsymbol{\Lambda}_k^{\rm n}$ where quaternion $\boldsymbol{\Lambda}_k^{\rm n}$ presents the SINS discrete noise. We are also assuming that column $\boldsymbol{\beta}_k \equiv \{\beta_k\}$ of the GDs measured angles and vector column $\boldsymbol{\omega}_k \equiv \{\omega_k\}$ (as the SINS discrete output) are accessible for forming the SC digital control.

3 The Problem Statement

For the SC body as a free solid with some simplifying assumptions we have the SC angular momentum (AM) vector $\mathbf{G}^o = \mathbf{J}\boldsymbol{\omega} + \boldsymbol{\mathcal{H}}(\boldsymbol{\beta}) \equiv \mathbf{0}$ and the conditions $\boldsymbol{\omega} = -\mathbf{J}^{-1}\boldsymbol{\mathcal{H}}(\boldsymbol{\beta})$, $\dot{\boldsymbol{\omega}} = \mathbf{w} = \mathbf{J}^{-1}\mathrm{M}^{\rm g}$. We consider principle problem on synthesis both a strict optimal and approximate optimal the SC gyromoment guidance laws which are calculated by explicit analytic relations. In the IRF $\mathbf{I}$ the SC's RM is described by kinematic relations for its BRF in the form

$$\dot{\boldsymbol{\Lambda}}(t) = \frac{1}{2}\boldsymbol{\Lambda}\circ\boldsymbol{\omega}(t); \dot{\boldsymbol{\omega}}(t) = \boldsymbol{\varepsilon} \equiv \mathbf{w}(t); \dot{\mathbf{w}}(t) = \mathbf{v} \quad (2)$$

during given time interval $\mathrm{T_p} \equiv [t_0^p, t_f^p]$ where $t_f^p \equiv t_0^p + T_p$. The optimization problem consists in determination of the time functions — quaternion $\boldsymbol{\Lambda}(t)$ and vectors $\boldsymbol{\omega}(t), \boldsymbol{\varepsilon}(t) \equiv \{\varepsilon_i(t)\}$ for general boundary conditions on left ($t = t_0^p$) and right ($t = t_f^p$) ends

$$\begin{aligned} &\boldsymbol{\Lambda}(t_0^p) = \boldsymbol{\Lambda}_0;\ \ \boldsymbol{\omega}(t_0^p) = \boldsymbol{\omega}_0;\ \ \mathbf{w}(t_0^p) = \mathbf{w}_0; \\ &\boldsymbol{\Lambda}(t_f^p) = \boldsymbol{\Lambda}_f;\ \ \boldsymbol{\omega}(t_f^p) = \boldsymbol{\omega}_f;\ \ \mathbf{w}(t_f^p) = \mathbf{w}_f \end{aligned} \quad (3)$$

with optimization of the integral quadratic criterion

$$\mathrm{I}_2 = \frac{1}{2}\int_{t_0^p}^{t_f^p} \langle \mathbf{v}(\tau), \mathbf{v}(\tau)\rangle\, d\tau \Rightarrow \min. \quad (4)$$

We study the dynamical properties of the flexible spacecraft and develop methods for synthesis of the SC attitude digital and pulse-width control.

4 Optimization of the Guidance Laws

4.1 Optimal one-axis motion

Of course, this problem is elementary and have analytic solution by Pontryagin's maximum principle. The SC optimal motion on criterion (4) with respect to any k axis is presented by the analytic function $\varphi_k(t)$ in a class of the five degree splines by normed time $\tau = (t - t_0^p)/T_p \subset [0, 1]$ with analytic relations

$$\varepsilon_k(\tau) = \varepsilon_k^0 + \tau(6a_3 + 12a_4\tau + 20a_5\tau^2)/T_p^2;$$

$$\omega_k(\tau) = \omega_k^0 + \varepsilon_k^0\,T_p\tau + \tau^2(3a_3 + 4a_4\tau + 5a_5\tau^2)/T_p;$$

$$\varphi_k(\tau) = \varphi_k^0 + \tau(\omega_k^0 T_p + \varepsilon_k^0 T_p^2\tau/2 + \tau^2(a_3 + a_4\tau + a_5\tau^2)),$$

where constant coefficients $a_s, s = 3 \div 5$ are defined by the vector-matrix relation

$$\begin{bmatrix} a_3 \\ a_4 \\ a_5 \end{bmatrix} = \begin{bmatrix} 10 & -4 & 0.5 \\ -15 & 7 & -1 \\ 6 & -3 & 0.5 \end{bmatrix} \begin{bmatrix} \varphi_k^f - \varphi_k^0 - \omega_k^0 T_p - \varepsilon_k^0 T_p^2/2 \\ T_p(\omega_k^f - \omega_k^0 - \varepsilon_k^0 T_p) \\ T_p^2\ (\varepsilon_k^f - \varepsilon_k^0) \end{bmatrix}$$

with given boundary conditions $\varphi_k^s, \omega_k^s, \varepsilon_k^s,\ s = 0, f$ for the elementary rotation.

4.2 Approximate optimal spatial motion

Developed analytical approach to the problem is based on necessary and sufficient condition for solvability of Darboux problem. At general case the solution is presented as result of composition by three ($k = 1 \div 3$) simultaneously derived elementary rotations of embeded bases $\mathbf{E}_k$ about units $\mathbf{e}_k$ of Euler axes, which positions are defined from the boundary conditions (3) for initial spatial problem. For all 3 elementary rotations with respect to units $\mathbf{e}_k$ the boundary conditions are analytically assigned. Into the IRF $\mathbf{I}$ the quaternion $\boldsymbol{\Lambda}(t)$ is defined by the production

$$\boldsymbol{\Lambda}(t) = \boldsymbol{\Lambda}_0 \circ \boldsymbol{\Lambda}_1(t) \circ \boldsymbol{\Lambda}_2(t) \circ \boldsymbol{\Lambda}_3(t), \quad (5)$$

where $\boldsymbol{\Lambda}_k(t) = (C_{\varphi_k(t)/2}, S_{\varphi_k(t)/2}\mathbf{e}_k)$ and functions $\varphi_k(t)$ present the elementary rotation angles in analytical form. Let us quaternion $\boldsymbol{\Lambda}^* \equiv (\lambda_0^*, \boldsymbol{\lambda}^*) = \tilde{\boldsymbol{\Lambda}}_0 \circ \boldsymbol{\Lambda}_f \neq \mathbf{1}$ have the Euler axis unit $\mathbf{e}_3 = \boldsymbol{\lambda}^*/S_{\varphi^*/2}$ for 3rd elementary rotation where angle $\varphi^* = 2\arccos(\lambda_0^*)$. For such rotations there are applied the boundary values

$$\begin{aligned} &\boldsymbol{\Lambda}_1(t_0^p) = \boldsymbol{\Lambda}_1(t_f^p) = \boldsymbol{\Lambda}_2(t_0^p) = \boldsymbol{\Lambda}_2(t_f^p) = \mathbf{1}; \\ &\boldsymbol{\Lambda}_3(t_0^p) = \mathbf{1};\ \ \boldsymbol{\Lambda}_3(t_f^p) = (C_{\varphi_3^f/2}, \mathbf{e}_3 S_{\varphi_3^f/2}), \end{aligned} \quad (6)$$

where $\varphi_3^f = \varphi^*$ and $\mathbf{1}$ is a single quaternion. For

$$\mathbf{e}_0^\omega \equiv \frac{\boldsymbol{\omega}_0}{\omega_0};\ \mathbf{e}_f^\omega \equiv \frac{\boldsymbol{\omega}_f}{\omega_f};\ \mathbf{e}_0^\varepsilon \equiv \frac{\boldsymbol{\varepsilon}_0}{\varepsilon_0};\ \mathbf{e}_f^\varepsilon \equiv \frac{\boldsymbol{\varepsilon}_0}{\varepsilon_0};\ \ a \equiv |\mathbf{a}|$$

unit $\mathbf{e}_1$ of 1st elementary rotation's on Euler's axis is selected by next simple algorithm:

$\mathbf{a} =: \mathbf{e}_0^\omega - \langle\mathbf{e}_0^\omega, \mathbf{e}_3\rangle\mathbf{e}_3, if\ a > 0, then\ \mathbf{e}_1 = \mathbf{a}/a, else$
$\mathbf{a} =: \mathbf{e}_f^\omega - \langle\mathbf{e}_f^\omega, \mathbf{e}_3\rangle\mathbf{e}_3, if\ a > 0, then\ \mathbf{e}_1 = \mathbf{a}/a, else$
$\mathbf{a} =: \mathbf{e}_0^\varepsilon - \langle\mathbf{e}_0^\varepsilon, \mathbf{e}_3\rangle\mathbf{e}_3,\ if\ a > 0, then\ \mathbf{e}_1 = \mathbf{a}/a, else$
$\mathbf{a} =: \mathbf{e}_f^\varepsilon - \langle\mathbf{e}_f^\varepsilon, \mathbf{e}_3\rangle\mathbf{e}_3,\ if\ a > 0, then\ \mathbf{e}_1 = \mathbf{a}/a,$
else 3rd rotation is only, e.g. $\boldsymbol{\Lambda}_1(t) = \boldsymbol{\Lambda}_2(t) \equiv \mathbf{1}$.

Unit $\mathbf{e}_2$ is defined as $\mathbf{e}_2 = \mathbf{e}_3 \times \mathbf{e}_1$. All vectors $\boldsymbol{\omega}_k(t) = \dot{\varphi}_k(t)\mathbf{e}_k$, $\boldsymbol{\varepsilon}_k(t) = \ddot{\varphi}_k(t)\mathbf{e}_k$ and $\dot{\boldsymbol{\varepsilon}}_k(t) = \dddot{\varphi}_k(t)\mathbf{e}_k$ have analytic form owing to functions $\varphi_k(t)$ which are optimal on criterion (4) for each elementary rotation.

The elaborated analytical technique of approximate optimization allows in addition to (3) the boundary condition $\mathbf{v}(t_f^p) \equiv \mathbf{v}_f$ with given vector $\mathbf{v}_f$ for a smooth conjugation of the rotational maneuver borders. Moreover, all elementary rotation angles are analytically presented in the form of six-degree splines of time. The analytic procedure was also elaborated for calculating the SC motion which is approximate optimal with respect to functional (4) with given restriction of the SC angular rate vector module ($|\boldsymbol{\omega}(t)| \leq \omega^*$) during its rotational maneuver. In this case, the elementary rotation functions are obtained by a smooth conjugation of the five-, one-, and six-degree splines of time (Somov, Ye. *et al.*, 2007, 2009*a*,*b*).

4.3 Optimal spatial motion

For nonlinear problem (2)–(4) Hamilton function is

$$H = -\tfrac{1}{2}\langle \mathbf{v}, \mathbf{v}\rangle + \tfrac{1}{2}\langle \mathrm{vect}(\tilde{\boldsymbol{\Lambda}} \circ \boldsymbol{\Psi}, \boldsymbol{\omega}\rangle + \langle \boldsymbol{\mu}, \boldsymbol{\varepsilon}\rangle + \langle \boldsymbol{\nu}, \mathbf{v}\rangle,$$

where associated quaternion $\boldsymbol{\Psi}(t) = \mathbf{C}_\varphi \circ \boldsymbol{\Lambda}(t), \mathbf{C}_\varphi = (\mathrm{c}_{\varphi 0}, \mathbf{c}_\varphi)$ is normed quaternion with $\mathbf{c}_\varphi = \{\mathrm{c}_{\varphi k}\}$. The associated differential system have the form

$$\dot{\boldsymbol{\Psi}} = \tfrac{1}{2}\boldsymbol{\Psi} \circ \boldsymbol{\omega}; \quad \dot{\boldsymbol{\mu}} = -\tfrac{1}{2}\tilde{\boldsymbol{\Lambda}} \circ \mathbf{c}_\varphi \circ \boldsymbol{\Lambda}; \dot{\boldsymbol{\nu}} = -\boldsymbol{\mu}.$$

The optimality condition $\partial H/\partial \mathbf{v} = -\mathbf{v} + \boldsymbol{\nu} = \mathbf{0}$ gives the optimal "control"

$$\mathbf{v}(t) = \mathbf{c}_\varepsilon - \mathbf{c}_\omega (t - t_0^p) + \tfrac{1}{2}\int_{t_0^p}^{t} (\int_{t_0^p}^{\tau} \tilde{\boldsymbol{\Lambda}}(s) \circ \mathbf{c}_\varphi \circ \boldsymbol{\Lambda}(s) ds) d\tau,$$

where vectors $\mathbf{c}_\varphi$, $\mathbf{c}_\omega = \{\mathrm{c}_{\omega k}\}$ and $\mathbf{c}_\varepsilon = \{\mathrm{c}_{\varepsilon k}\}$ must be numerically defined using known analytical structure of solution for direct system (2) and taking into account the boundary conditions (3). Standard Newton iteration method was applied for numerical obtaining the "control" $\mathbf{v}(t)$ which is a strict optimal on index (4) for the nonlinear optimization problem (2) – (4). Moreover analytical solution of the "start" problem (initial point) was applied in the form of approximate optimal motion (5) with the constant vectors $\mathbf{c}_\varphi$, $\mathbf{c}_\omega$ and $\mathbf{c}_\varepsilon$. Values of these constant vectors are numerically corrected by an iteration procedure using a combine numerical integration of direct and associated differential systems which are linearizated at neighbourhood of numerical solution on previous iteration. At such initial point the Newton's iteration process have a rapid convergence: usually there is needed only 2 – 3 iterations for obtaining a numerical solution with fine accuracy. Difference between approximate and strict optimal spatial motion is very light on criterion (4) – up to 5 % for the SC practical rotational maneuvers.

5 The GMC digital control

Of course, own dynamical properties of the information mini-satellites essentially depend on the SC mechanical characteristics. We consider such SC with general mass m=400 kg and next the GMC parameters:

$$\mathbf{J} = \begin{bmatrix} 50 & -5 & 0 \\ -5 & 130 & 0 \\ 0 & 0 & 100 \end{bmatrix}; \begin{array}{l} \lceil a_j^q \rfloor = \lceil 25.67, 28.94, 22.54 \rfloor; \\ \lceil \Omega_j^q \rfloor = \lceil 0.8, 2.2, 3.6 \rfloor; \\ \delta^q = 0.005; J_g = 0.04; H = 2. \end{array}$$

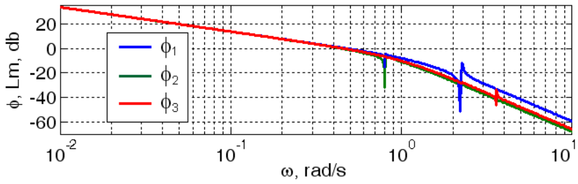

Figure 5. The spacecraft continuous LAFC on channels

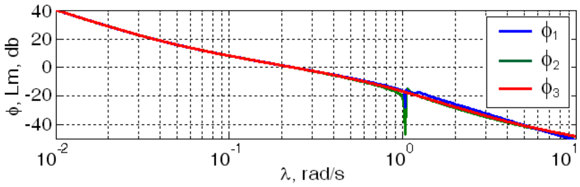

Figure 6. The discrete LAFC of the SC open-loop channels

For these parameters the gyromoment system have own *nutation* frequencies $(\Omega_i^n) = (1.42, 0.88, 1)$ rad/s at the SC attitude channels, therefore at a choice of the GD damping coefficients $b_i^g = 2\xi\Omega_i^n J_g$ with $\xi = 0.8$ the GMC have perfect damping properties by a gyromoment coupling its motion with the SC structure oscillations (Somov, Ye. *et al.*, 2005). The logarithmic amplitude frequency characteristics (LAFC) on channels of the flexible SC as a continuous plant are presented in Fig. 5. Into the control loop a discrete error signal quaternion is $\mathbf{E}_k = (e_{0k}, \mathbf{e}_k) = \tilde{\boldsymbol{\Lambda}}_k^p \circ \boldsymbol{\Lambda}_k^{\mathrm{m}}$ and the SC attitude mismatch vector is $\boldsymbol{\varepsilon}_k = \delta\boldsymbol{\phi}_k = \{\delta\phi_{ik}\} = \{-2e_{0k}e_{ik}\}$. Elaborated the GMC nonlinear digital control law $\mathbf{m}_k^g(\boldsymbol{\varepsilon}_k, \boldsymbol{\beta}_k, \boldsymbol{\omega}_k^p, \boldsymbol{\omega}_k^{\mathrm{e}}) \equiv \{m_{ik}^g\}$ have the simple recurrent form

$$\begin{aligned} \mathbf{g}_{k+1} = \mathbf{g}_k + \boldsymbol{\varepsilon}_k; \ \mathbf{m}_k^g = -\mathbf{A}_{\mathrm{H}}^{\mathrm{t}}(\boldsymbol{\beta}_k)\boldsymbol{\omega}_k^{\mathrm{g}}; \\ \boldsymbol{\omega}_k^{\mathrm{g}} = \boldsymbol{\omega}_k^p - \boldsymbol{\omega}_k^{\mathrm{e}} + \mathbf{K}^g(\boldsymbol{\varepsilon}_k + a_g \mathbf{g}_k), \end{aligned} \tag{7}$$

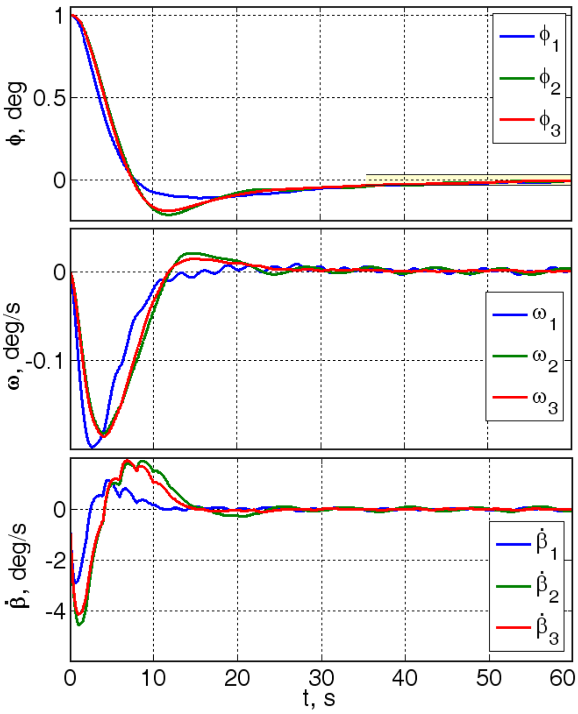

Figure 7. Transient processes at the SC digital stabilization

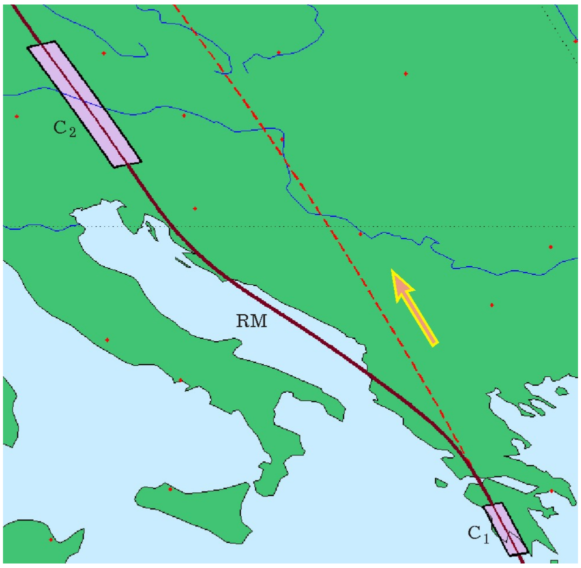

Figure 8. The space land-survey with two observation courses

where vector $\boldsymbol{\omega}_k^{\mathrm{e}}$ is intended for compensation of the CEU vector torque at the GMC unloading from accumulated angular momentum, matrix $\mathbf{K}^g = \lceil k_i^g \rfloor$ and the constant parameter $a_g = T_u/T_{\mathrm{I}}$. Fig. 6 presents the discrete LAFC of the SC open-loop channels with the GMC digital control law (7) for values $k_i^g = 0.25$, $T_u = 2$ s and $T_{\mathrm{I}} = 22$ s. Transient processes into close-loop system for the flexible SC attitude stabilization by the GMC nonlinear digital control law are presented in Fig. 7. Here initial the SC attitude is $\phi_i(0) = 1$ deg but initial conditions are zero for other variables, the GD parameters $\dot{\beta}_g^{\mathrm{o}} = 5\;10^{-6}$ rad/s and $m_g^{\mathrm{f}} = 10^{-3}$ Nm are applied and gaussian discrete noise have the standard deviation $\sigma^{\mathrm{m}} = 10$ arc sec at the SC attitude measuring, as it is defined by the quaternion $\boldsymbol{\Lambda}_k^{\mathrm{m}}$. One can see in Fig. 7 that the transient processes have very well characteristics and settle time is ≈ 30 s.

The GMC digital control law was researched for a land-survey mini-satellite onto the sun-synchronous orbit with altitude 600 km. In Fig. 8 one can see the SC trace (dotted line), first course C_1 at the trace scanning observation into the nadir direction, the line-of-sight track at the SC rotation maneuver (RM) and second course C_2 for next the trace scanning observation but with the line-of-sight angular deflection on 30 deg. at the SC roll channel. For this studied problem we have next boundary conditions:

$t = 0s: \boldsymbol{\Lambda}^p = (0.542909, 0.267808,$
$-0.716157, -0.347344) \Rightarrow \boldsymbol{\phi} = \{3.04, 0., 0.\}^{\circ};$
$\boldsymbol{\omega}^p = \{-0.00243185, 0.00329356, 0.06196994\}^{\circ}/s.$

$t = 20s: \boldsymbol{\Lambda}^p = (0.547115, 0.26009,$
$-0.718529, -0.341665) \Rightarrow \boldsymbol{\phi} = \{2.99, 0., 0.\}^{\circ};$
$\boldsymbol{\omega}^p = \{-0.002432228, 0.00329356, 0.06196994\}^{\circ}/s.$

$t = 180s: \boldsymbol{\Lambda}^p = (0.746515, 0.271421,$
$-0.556874, -0.242771) \Rightarrow \boldsymbol{\phi} = \{1.82, 29.98, -1.05\}^{\circ};$
$\boldsymbol{\omega}^p = \{-0.03357431, 0.00197426, 0.05370893\}^{\circ}/s.$

$t = 240s: \boldsymbol{\Lambda}^p = (0.758302, 0.242608,$
$-0.559189, -0.231141) \Rightarrow \boldsymbol{\phi} = \{1.83, 29.98, -1.05\}^{\circ};$
$\boldsymbol{\omega}^p = \{-0.033713393, 0.001826071, 0.05371511\}^{\circ}/s.$

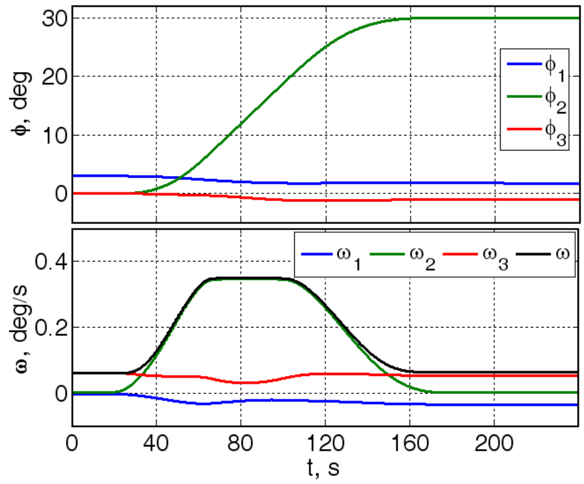

Figure 9. The attitude guidance program at land-survey

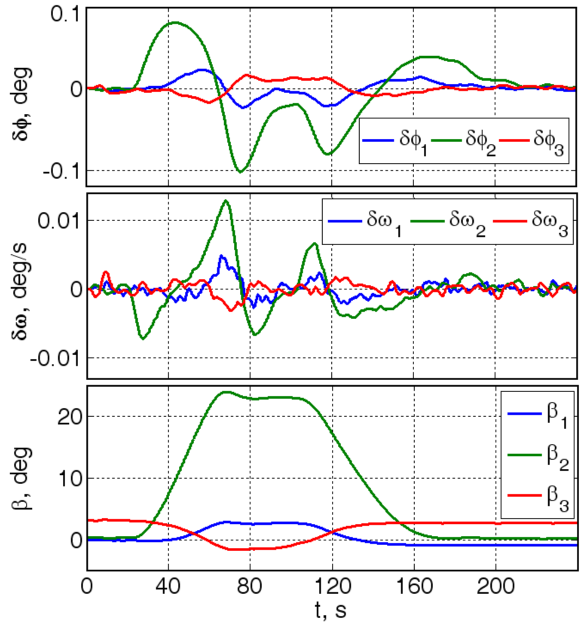

Figure 10. The SC attitude errors and the GD's angles

The SC guidance program was calculated taking into account the restriction $|\boldsymbol{\omega}(t)| \leq \omega^* = 0.35$ deg/s, results are presented in Fig. 9. The SC attitude errors at 1st course $\mathrm{C}_1(t \in [0, 20)$s), the RM ($t \in [20, 180)$s), 2nd course $\mathrm{C}_2(t \in [180, 240]$s) and the GD's angles $\beta_i(t)\;\forall t \in [0, 240]$s are presented in Fig. 10.

6 The CEU pulse-width control

The Combine Engine Unit (CEU) contains eight EREs (see Fig. 4) with the PWM of their thrusts on the period T_r^{e} and is applied for forming $\forall t \in [t_r, t_r + T_u^{\mathrm{e}})$ the force vector $\mathbf{R}^{\mathrm{e}}(t) = \Sigma \mathbf{P}_p(t)$ and the torque vector $\mathbf{M}^{\mathrm{e}}(t) = \Sigma \mathbf{M}_p(t)$ into the BRF. We introduce the denotations: $\boldsymbol{\tau}_r = \{\tau_{pr}\}$; $\rho = (b_x^2 + b_y^2 + b_z^2)^{1/2}$;

$$\mathbf{r}_p = \boldsymbol{\rho}_p/\rho;\; \mathbf{D}^{\mathrm{e}} = -\{[\mathbf{e}_p], [\mathbf{r}_p \times \mathbf{e}_p]\};\; \tilde{\mathbf{r}}^{pg} = \mathbf{R}^{pg}/\mathrm{P}^{\mathrm{m}};$$

$$\tilde{\mathbf{m}}^{pg} = \mathbf{M}^{pg}/(\mathrm{P}^{\mathrm{m}}\,\rho);\quad \mathbf{t}^{pg} \equiv \{\tilde{\mathbf{r}}^{pg}, \tilde{\mathbf{m}}^{pg}\},$$

where $\mathbf{R}^{pg}$ and $\mathbf{M}^{pg}$ are *given pulses* of the vectors $\mathbf{R}^{\mathrm{e}}$ and $\mathbf{M}^{\mathrm{e}}$ presented into the BRF.

Principle problem is that: how to solve the equation $\mathbf{D}^{\mathrm{e}}\boldsymbol{\tau}_r = \mathbf{t}_r^{pg}$, where $\boldsymbol{\tau}_r \in \bar{\Re}_+ \subset \mathbb{R}_+^8$, $\mathbf{t}_r^{pg} \in \mathbb{R}^6$, with

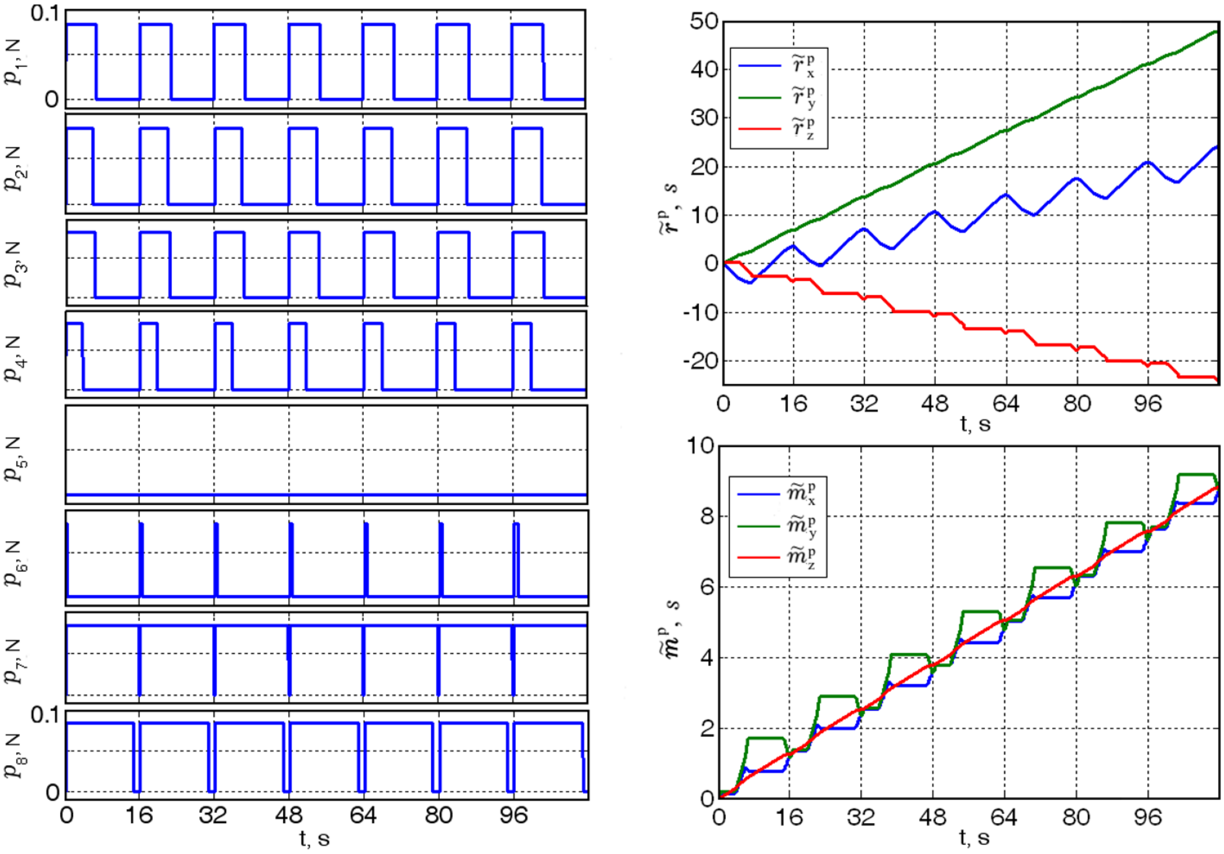

Figure 11. The time diagrams of current the ERE thrusts and the CEU normed pulses of force and torque

respect to the column $\boldsymbol{\tau}_r = \{\tau_{pr}\}$ and with the condition $0 \leq \tau_{pr} \leq T_u^{\mathrm{e}} \; \forall p = 1 \div 8$ when matrix $\mathbf{D}^{\mathrm{e}}$ and column $\mathbf{t}_r^{pg}$ are given ?

At denotation $(\mathbf{D}^{\mathrm{e}})^{\#} = (\mathbf{D}^{\mathrm{e}})^{\mathrm{t}}(\mathbf{D}^{\mathrm{e}}\,(\mathbf{D}^{\mathrm{e}})^{\mathrm{t}})^{-1}$ elaborated law for the CEU ELE's trust distribution have the simple algorithmic form:

$$\hat{\boldsymbol{\tau}}_r \equiv \{\hat{\tau}_{pr}\} = (\mathbf{D}^{\mathrm{e}})^{\#}\, \mathbf{t}_r^{pg}; \quad \tilde{\tau}_{pr} =: \hat{\tau}_{pr} - \min(\hat{\tau}_{pr});$$

$$if \quad \max(\tilde{\tau}_{pr}) > T_u^{\mathrm{e}} \quad then \quad \tau_{pr} = \tilde{\tau}_{pr} T_u^{\mathrm{e}} / \max(\tilde{\tau}_{pr}).$$

Fig. 11 presents results of the CEU work's simulation for the CEU parameters $\tau_{\mathrm{m}} = 0.25$ s; $T_u^{\mathrm{e}} = 16$ s; $b_x = 1$ m, $b_y = 0.7$ m, $b_z = 0.6$ m; $\alpha^{\mathrm{e}} = \pi/3$, $\beta^{\mathrm{e}} = \pi/6$ at the ERE's thrust value $\mathrm{P}^{\mathrm{m}} = 0.083$ N and given pulses $\mathbf{R}^{pg} = \{2, 4, -2\}$ Ns, $\mathbf{M}^{pg} = \{1, 1, 1\}$ Nms.

7 Software for Research and Design

The *SIRIUS-S* software system is intended for modeling, research, simulation, animation and development of functional requirements to the gyromoment control systems of the land-survey SC allowing to find main factors affecting on the SC design characteristics. The system includes a dialogue monitor, the modeling, analysis and synthesis subsystems, and also the simulation and animation subsystems. It is based on well-known *Matlab* system and animation *Blender* package (Mullen, 2011), and also uses the core concepts of computer interactive graphics with full integration of the Windows *OpenGL* (Angel, 2002) and an emphasis on application-based programming, details see in Somova (2012). Presented in Fig. 2 land-survey satellite is equipped by a telescope with removing cover, 4 star trackers, the GMC based on 4 gyrodines, 8 low-trust electro-reaction engines and 4 moving solar array panels. Fig. 12 presents an animation frame at a scanning space observation by this satellite.

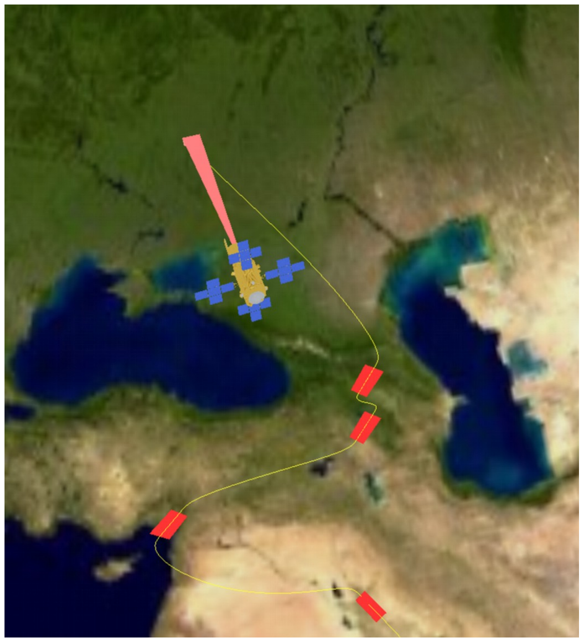

Figure 12. An animation frame at the Earth scanning observation

Conclusion

The optimization problem on attitude guidance of the information mini-satellites were put forward and elaborated methods for solving the problem were presented. Some results on dynamic synthesis of the SC attitude robust digital control by the GMC with three gyrodines and pulse-width control by the CEU with eight electro-reaction engines were represented. These results were obtained by the *SIRIUS-S* software system (Somov *et al.*, 2011, 2012, 2013; Somov, Ye. *et al.*, 2013*a*,*b*).

Acknowledgements

The work was supported by the RFBR (Grants 11-08-01037 and 13-08-97000) and by Division on EMMCP of Russian Academy of Sciences (Program 14).

References

Angel, E. (2002). *Interactive Computer Graphics: A Top-Down Approach Using OpenGL*. 3rd ed.. Addison Wesley. Boston.

Helvajian, H. and S.W. Jonson (2009). *Small Satellites: Past, Present and Future*. The Aerospace Press, AIAA.

Kramer, H.J. (2002). *Observation of the Earth and Its Environment. Survey of Missions and Sensors*. 4th ed.. Springer.

Mullen, T. (2011). *Introducing Character Animation with Blender*. 2nd ed.. B&W Publishing. Edinburgh.

Somov, S. (2007). Modeling of a flexible satellite motion. *Actual Problems of Aviation and Aerospace Systems* **12**(3(25)), 85–93.

Somov, S. (2010). Guidance and robust pulse-width control of an information satellite at initial modes. In: *Proceedings of 18th IFAC Symposium on Automatic Control in Aerospace http://www.ifac-papersonline.net/Detailed/47393.html*. Nara. pp. 1–6.

Somov, S. (2012*a*). Pulse-width control of magnetic and reaction drivers at unloading a satellite's gyro moment cluster. In: *Proceedings of 10th International Chetayev Conference on Analytical Mecha-nics, Stability and Control*. Vol. 3/II. Kazan. pp. 364–367.

Somov, S. (2012*b*). Spacecraft attitude pulse-width control at initial, service and emergency modes. In: *AIP Conference Proceedings Ser.*. Vol. 1493. American Institute of Physics, http://dx.doi.org/10.1063/1.4765600. pp. 933–940.

Somov, S., S. Butyrin and T. Somova (2012). Computer technologies for optimization, simulation and animation of observation satellite spatial motion. In: *Proceedings of 9th IFAC Symposium on Advances in Control Education http://www.ifac-papersonline.net/Detailed/52853.html*. Nizhny Novgorid. pp. 155–159.

Somov, S., S. Butyrin and T. Somova (2013). Simulation technologies for long-term target planning and in-flight management of the spacecraft control systems. In: *Proceedings of IFAC Conference on Manufacturing Modeling, Management, and Control*. Saint Petersburg. pp. 1278–1283.

Somov, S., Ye. Somov, S. Butyrin and A. Butko (2011). Optimizing the guidance and control laws at space optoelectronic observation. In: *Proceedings of 18th IFAC Congress http://www.ifac-papersonline.net/Detailed/48161.html*. Milan. pp. 2078–2083.

Somov, Ye. (1992). Dynamics of the multiple digital gyromoment system for spatial stabilization of a flexible spacecraft. In: *Spacecraft Dynamics and Control*. pp. 46–76. Nauka. Novosibirsk. In Russian.

Somov, Ye., H. Siguerdidjane and V. Rutkovsky (2012). Postgraduate education and new challenges on stability and adaptive-robust control in aerospace. In: *Proceedings of 9th IFAC Symposium on Advances in Control Education http://www.ifac-papersonline.net/Detailed/52907.html*. Nizhny Novgorid. pp. 312–317.

Somov, Ye., S. Butyrin and S. Somov (2005). Coupling and damping the structure oscillations at spacecraft gyromoment digital control. In: *Proceedings of 1st International Scientific Conference on Physics and Control*. Saint Petersburg. pp. 497–502.

Somov, Ye., S. Butyrin and S. Somov (2009*a*). Guidance and control of a land-survey spacecraft with smooth conjugation of boundary conditions. In: *Proceedings of 4th International Scientific Conference on Physics and Control http://lib.physcon.ru/doc?id=11d5d7ece0b5*. Catania.

Somov, Ye., S. Butyrin and S. Somov (2009*b*). Spacecraft guidance and robust attitude control with precise pointing the flexible antennas. In: *Proceedings of 18th IEEE International Conference on Control Applications. Part of 3rd IEEE Multi-conference on Systems and Control http://ieeexplore.ieee.org/xpl/freeabs_all.jsp?arnumber=5281102*. Saint Petersburg. pp. 1057–1062.

Somov, Ye., S. Butyrin and S. Somov (2013*a*). Economical attitude and orbit control of information satellites by electromechanical, magnetic and plasma drivers. In: *Proceedings of 6th International Conference on Recent Advances in Space Technologies*. Istanbul. pp. 1009–1014.

Somov, Ye., S. Butyrin, S. Somov and G. Anshakov (2007). Guidance and robust gyromoment attitude control of agile flexible remote sensing spacecraft. In: *Proceedings of 17th IFAC Symposium on Automatic Control in Aerospace http://www.ifac-papersonline.net/Detailed/38694.html*. Toulouse. pp. 1–6.

Somov, Ye., S. Butyrin, S. Somov and T. Somova (2013*b*). SIRIUS-S software environment for computer-aided designing of attitude control systems for small information satellites. In: *Proceedings of XX Saint Petersburg International Conference on Integrated Navigation Systems*. Saint Petersburg. pp. 325–328.

Somova, T. (2012). Simulation and animation of spatial motion of a maneuvering land-survey satellite. *Izvestiya of Samara Scintific Centre, Russian Academy of Sciences* **14**(6), 125–128. In Russian.